

# Fabrication of UV-curable waterborne fluorinated polyurethane-acrylate and its application for simulated iron cultural relic protection

Jicheng Xu, Yan Jiang, Tao Zhang, Yuting Dai, Dongya Yang, Fengxian Qiu, Zongping Yu, Pengfei Yang

© American Coatings Association 2018

**Abstract** In this study, UV-curable waterborne fluorinated polyurethane-acrylate (UV-WFPUA) coatings were investigated to evaluate their potential application for protecting iron cultural relics. A series of UV-WFPUA materials were synthesized with different contents of hexafluorobutyl methacrylate (HFBMA) and characterized by Fourier transform infrared spectroscopy and scanning electron microscopy. When the content of HFBMA was 10%, the UV-WFPUA-3 material exhibited good mechanical properties and excellent hydrophobicity. The iron sheet was selected to simulate an iron artifact sample in this study. The obtained results indicated that the prepared UV-WFPUA material could provide excellent protective properties for simulated iron artifacts.

**Keywords** Cultural relics, Iron artifacts, UV-curable, Waterborne fluorinated polyurethane-acrylate

## Introduction

Cultural heritage is a precious treasure from history because it conveys information about social and cultural backgrounds and represents a bridge between

contemporary society and the past, which is important for studying human civilization.

Regardless of their nature, artifacts are exposed to several degradation agents including physical erosion, chemical degradation, temperature stresses, humidity cycles, exposure to light and microorganisms, accounting for the natural aging of materials.<sup>1</sup> Moreover, anthropic activities increase the concentration of SO<sub>2</sub>, NO<sub>x</sub>, and VOC (volatile organic compound) gases in the atmosphere, which eventually increase the rate of corrosion and degradation of cultural heritage materials.<sup>2</sup> Some cultural relics are so fragile that they cannot leave the carefully controlled light,<sup>3</sup> humidity, and temperature conditions of their storage environments. Therefore, one of the most important issues for cultural relic conservation is protective materials,<sup>4</sup> which must comply with some important constraints (i.e., reversibility, inertness, and maintenance of the integrity of the original items).<sup>5,6</sup>

Recently, the conservation of cultural heritage has become a hot research topic that has attracted the attention of scientists worldwide.<sup>7,8</sup> Iron cultural relics, which have been of excellent value in science, art, and history, are important cultural artifacts. Most ancient weapons have been cast from iron including swords, machetes, and shields. Iron cultural relics are composed of iron-carbon alloys, where the major ingredient (Fe element) is typically easily eroded due to its active chemical properties. Environmental conditions can substantially affect iron materials, and therefore, conservation and restoration of iron cultural heritage items are currently very important areas. Degradation phenomena are more prominent in the field of cultural heritage where iron materials have been exposed to environmental conditions for prolonged time periods. Major pollutants that seriously affect iron artifacts include water, carbon, nitrogen, and sulfur oxides, along with aerosol particulate matter,<sup>9</sup> moist environments and acidic soil that cause electrochemical

---

J. Xu, Y. Jiang  
Zhenjiang Key Laboratory of Functional Chemistry,  
Institute of Medicine & Chemical Engineering, Zhenjiang  
College, Zhenjiang 212003, China

J. Xu, T. Zhang, Y. Dai, D. Yang, F. Qiu (✉)  
School of Chemistry and Chemical Engineering, Jiangsu  
University, Zhenjiang 212013, China  
e-mail: fxqiuchem@163.com

Z. Yu, P. Yang  
Suzhou Mingda Macromolecule Science and Technology  
CO., Ltd, Suzhou 215234, China

corrosion and are primarily responsible for surface corrosion.<sup>10</sup> In general, corrosion occurs at the surface of iron materials and can penetrate further into their bulk.<sup>11</sup> The protection of cultural heritage via surface treatment with polymers is a customary method due to its capacity to form a pyknotic protective layer on the material surface and to control the transport of different corrosion products from the surface to the interior.<sup>12</sup>

Waterborne polyurethane is an ideal preparation of an environmentally friendly waterproof coating material due to its low toxicity as well as mechanical and nonpolluting properties.<sup>13–17</sup> Waterborne polyurethane-acrylate (WPUA) as well as polyacrylic resins (PA) possess cauterization abilities and excellent gloss. The UV-curable waterborne polyurethane-acrylate system is typically composed of a reactive waterborne polyurethane-acrylate oligomer (prepolymer), reactive diluents, and a photoinitiator.<sup>18,19</sup> The fluorinated acrylate copolymer emulsion possesses hydrophobic, oleophobic, and antifouling properties.<sup>20,21</sup> The arrangement of fluorine atoms on the outmost surface of the films plays a key role in achieving excellent hydrophobicity and low surface free energy for the treated material surface.<sup>22</sup> In recent years, fluoropolymer has been widely used in coating, fabric finish, leather, and packing areas.<sup>23</sup>

Cultural relic protective coatings must meet several special requirements for successful application including good adhesion, mechanical and physical durability, good aesthetic appearance, transparency,<sup>24</sup> chemical inertness, impermeability, solvent and acid resistance, good friction and antiwear properties, long-term stability and reversibility.<sup>25</sup> Few studies or reviews on iron artifact restoration have been reported. Therefore, novel methods or materials should be explored for the restoration and protection of iron artifacts. A novel cultural relic protective coating that combines UV-curable technology, waterborne polyurethane, and fluorine material advantages will have a broad range of potential applications.

In this study, a series of UV-curable waterborne fluorinated polyurethane-acrylate (UV-WFPUA) coatings were prepared via the introduction of different amounts of hexafluorobutyl methacrylate (HFBMA). The properties and structures of the UV-WFPUA materials were characterized based on tensile strength, elongation at break, and contact angle measurements

as well as thermogravimetric analysis (TGA), Fourier transform infrared (FTIR) spectroscopy, and X-ray diffraction (XRD). The results indicated that the UV-WFPUA-3 film should exhibit satisfactory mechanical properties, water resistance, acid resistance, and thermal stability. Iron sheets were prepared to simulate the surface composition and morphology of iron cultural relics. The UV-WFPUA-3 coating was chosen to protect the iron sheet, and the protective effect was satisfactory. The obtained results indicated that the prepared UV-WFPUA material met the requirements for iron preservation. In addition, the new UV-WFPUA materials exhibited long-lasting protection, high physicochemical properties, and simplicity in application and are more economical.

## Experimental

### Materials

The self-made waterborne polyurethane-acrylate (WPUA) oligomer was used in our previous studies.<sup>26</sup> The photoinitiator Darocur 1173 and tripropyleneglycol diacrylate (TPGDA) were obtained from Mingda Macromolecule Science and Technology Co., Ltd., Suzhou, China, and used as the reactive diluents and initiators, respectively. The 2,2,3,4,4-Hexafluorobutyl methacrylate (HFBMA) was supplied by Xuejia Fluorine-Silicon Chemical Co., Ltd., Harbin, China.

### Preparation of UV-curable coating

The self-made WPUA oligomer was successfully prepared according to our previous study. The WPUA oligomer, HFBMA monomer, reactive diluents (TPGDA), and Darocur 1173 photoinitiator were added into a beaker followed by stirring; and the specific formulation is provided in Table 1. In this study, a series of UV-WFPUA coatings were obtained according to the recipe.

The UV-WFPUA coating samples were placed onto a poly (tetrafluoroethylene) film plate at ambient temperature for approximately 6 h until the UV-WFPUA emulsion was barely able to flow. Then, the sample was transferred into an ultraviolet curing

**Table 1: Basic recipe for UV-curable coatings**

	Sample	Oligomer (%)	Monomer (%)		Photoinitiator (%) Darocur 1173
			HFBMA	TPGDA	
1	UV-WFPUA-1	80	0	17	3
2	UV-WFPUA-2	75	5	17	3
3	UV-WFPUA-3	70	10	17	3
4	UV-WFPUA-4	65	15	17	3
5	UV-WFPUA-5	60	20	17	3

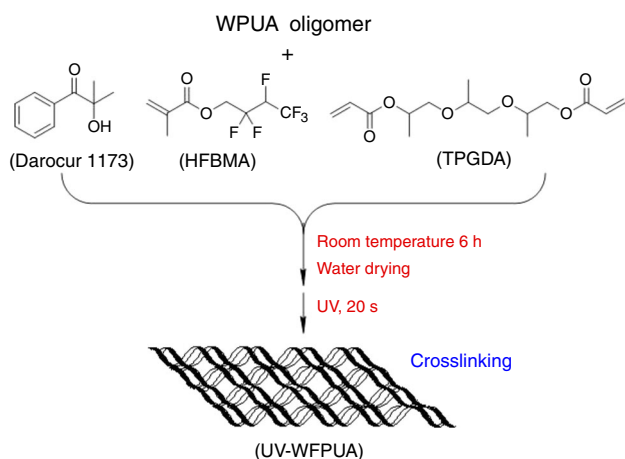


**Fig. 1: Formation of the UV-WFPUA coating film**

machine equipped with a UV lamp with a main wavelength of 365 nm, the distance to the center of the UV lamp was 20 cm, and the UV energy was 1000 J/s. The photoinitiator was activated immediately and produced active free radicals due to the UV light, which resulted in the reaction of TPGDA with the double bond of the monomers and oligomer in the prepolymer. Therefore, the UV-WFPUA films were obtained after a few seconds. The formation process for a series of UV-WFPUA coating films is shown in Fig. 1.

### Characterization

The hardness, tensile strength, and elongation at break of the UV-WFPUA films were measured using a test instrument (KYLX-A and KY-8000A, Jiangdu Kaiyuan Test Machine Co., Ltd., China). The tensile strength and elongation at break of each dumbbell UV-WFPUA film specimens were tested at a speed of 50 mm/min, and each dumbbell film specimen was 0.2 cm long at two ends, 0.2 mm thick and 4 mm wide at the neck. Each sample was tested 3 times, and the average value was computed.

The UV-WFPUA film samples were immersed in toluene for 48 h after the samples (2 cm × 2 cm) were weighed. Then, the samples were removed and dried in a dryer at room temperature until a constant-weight specimen was obtained. The gel content of the sample was calculated using the following formula (1):

$$G = \frac{W}{W_0} \times 100\% \quad (1)$$

where  $W_0$  and  $W$  are the mass of the UV-WFPUA film samples before being immersed into toluene and after being dried, respectively.

The UV-WFPUA films were weighed prior to being placed into the reagent bottle, which was filled with deionized water, 3.0% HCl and ethanol at room

temperature, and marked as  $m_1$ . All films were removed after 24 h, weighed and marked as  $m_2$ . The water absorption or swelling degree ( $\omega$ ) was calculated using the following formula (2):

$$\omega = \frac{m_2 - m_1}{m_1} \times 100\% \quad (2)$$

The contact angle measurement of the UV-WFPUA films was carried out on a commercial video-based contact angle measuring device (KSV Instruments Ltd., Finland). Different locations on the same sample were measured, and the average value was calculated.

The chemical components of the UV-WFPUA films were characterized by FTIR spectroscopy (AVATAR 360, Nicolet, Madison, USA) from 4000 to 400  $\text{cm}^{-1}$ .

The morphology of the UV-WFPUA films was characterized using a scanning electron microscope (S-4800, Hitachi Corp., Japan).

One thin rectangular (5 cm × 2.5 cm) iron sheet was chosen as a simulation sample of an iron relic. The rectangular iron sheet was rubbed with fine sandpaper and washed with distilled water followed by drying in an oven. The iron sheet was halved, one iron sheet was coated with the UV-WFPUA-3 emulsion and irradiated under ultraviolet (the light source is the same as that described in section “Preparation of UV-curable coating”) for 30 s, and the other iron sheet consisted of the naked surface for comparison. Both iron sheets were exposed to outdoor conditions for several days. The corrosive state of the simulated iron cultural relic iron sheets was observed with the naked eye and photographed.

## Results and discussions

### Effect of different HFBMA content on the mechanical properties of the UV-WFPUA films

The mechanical properties of the UV-WFPUA films were tested by measuring the hardness, tensile strength, and elongation at break. As shown in Table 2, the hardness of the UV-WFPUA films increased as the HFBMA content increased. This phenomenon may be due to the form of the fluorinated monomer being hard segments in this waterborne polyurethane material. As the HFBMA monomer content increased, the ratio of hard segments increased, and the pliability of the UV-WFPUA films decreased. As shown in Table 2, the elongation at break decreased, and the tensile strength increased as the HFBMA content increased, which may be due to the electronegativity of F being relatively higher, and the rigidity of the molecular chain was reinforced. Moreover, the hydrogen bonding interaction was stronger upon introduction of F, which resulted in an increase in the tensile strength and a decrease in the elongation at break.<sup>27</sup>

**Table 2: Mechanical properties of the UV-WFPUA films**

Sample	Hardness (shore A)	Tensile strength (MPa)	Elongation at break (%)
UV-WFPUA-1	90.3	4.99	24.58
UV-WFPUA-2	91.7	5.13	18.90
UV-WFPUA-3	92.2	5.27	18.02
UV-WFPUA-4	93.3	5.56	17.34
UV-WFPUA-5	93.9	6.48	13.16

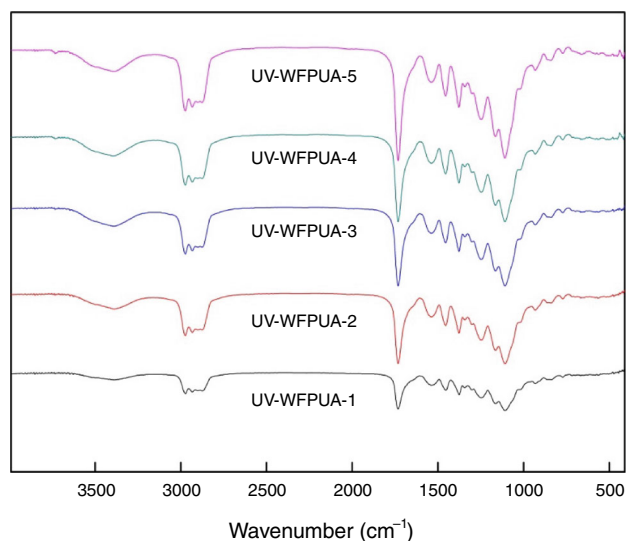
**Table 3: Gel content and water absorption (or swelling degree) of the UV-WFPUA films**

Sample	Gel content (%)	Water absorption (%)	Swelling degree (%)	
			HCl (3%)	Ethanol
UV-WFPUA-1	92.25	8.41	5.34	28.40
UV-WFPUA-2	92.66	5.73	2.88	25.08
UV-WFPUA-3	93.04	4.81	2.68	24.24
UV-WFPUA-4	94.30	4.43	2.46	20.64
UV-WFPUA-5	94.65	4.13	2.29	18.39

### ***Effect of the HFBMA content on the gel content and water absorption (or swelling degree) of UV-WFPUA films***

The gel content and water absorption (or swelling degree) of the UV-WFPUA films are listed in Table 3. As shown in Table 3, UV-WFPUA-1 exhibited the lowest gel content, and as the HFBMA content increased, the gel content in the UV-WFPUA films increased, indicating that a higher HFBMA content results in a higher double bond conversion. In addition, a higher gel rate in the film results in a higher crosslinking density.

Based on the results in Table 3, the water absorption of UV-WFPUA-1 was 8.41%. This result may be due to dihydroxymethyl butyric acid (DMBA), which is one of the main ingredients in the WPUA oligomer and contains a large number of hydrophilic groups.<sup>28</sup> When HFBMA was added to the system, the water absorption significantly decreased, and the water absorption of the UV-WFPUA-3 films was only 4.81%. When the content of HFBMA was further increased, the rate of the decrease in the water absorption of the films decreased. This result is mainly because the fluorine on the film surface had gradually reached a balance due to migration and enrichment, the amount of fluorine on the film surface was not significantly increased any more, water absorption of UV-WFPUA films was no longer significantly decreased. The addition of excess fluorine leads to other problems, such as cost increases and environmental hazards. Therefore, when the content of HFBMA was 10%, the combined effect was optimal. In addition, the swelling degrees (HCl or ethanol) of the UV-WFPUA films were lower than that of UV-WFPUA-1 (HFBMA, 0%), indicating that the interior and surface structure improved after introduction of HFBMA.

**Fig. 2: FTIR spectra of the UV-WFPUA films**

### ***Structural characterization of the UV-WFPUA films***

The FTIR spectra of the UV-WFPUA films are shown in Fig. 2. As shown in Fig. 2, the characteristic absorption peaks of the  $-NCO$  bond disappeared in the five UV-WFPUA film samples, indicating that IPDI had reacted completely. Furthermore, the typical characteristic stretching peak of  $N-H$  ( $\nu_{N-H}$ ) was observed at  $3340\text{ cm}^{-1}$ . The stretching vibration absorption peaks of  $C=O$  ( $\nu_{C=O}$ ) at  $1730\text{ cm}^{-1}$  and  $N-H$  ( $\delta_{N-H}$  and  $\nu_{C-H}$ ) at  $1540\text{ cm}^{-1}$ , which corresponded to the carbonyl group of the urethane, were also observed. In contrast to the spectra of the UV-WFPUA-1 film, new characteristic absorption peaks of

$-\text{CF}_3$  at  $1242\text{ cm}^{-1}$  and  $-\text{CF}_2-$  at  $1165\text{ cm}^{-1}$  were observed. In addition, peaks corresponding to  $-\text{CF}_2-$  at  $1165\text{ cm}^{-1}$  and bands corresponding to the ester carbonyl ( $\text{O}-\text{C}-\text{O}$ ) at  $1150\text{ cm}^{-1}$  overlapped.<sup>29</sup> Additionally, the rocking and wagging vibration peaks of  $-\text{CF}_3$  at  $659\text{ cm}^{-1}$  appeared, indicating the fluorine-containing groups reacted in the system. As the HFBMA content increased, the characteristic absorption peaks of  $-\text{CF}-$  at  $1076\text{ cm}^{-1}$  became more intense. The results indicated that the UV-WFPUA films had been successfully synthesized.

### Effect of the HFBMA content on the contact angle of the UV-WFPUA films

Copolymers with long fluorinated side chains can effectively contribute to lowering the surface free energy of materials, which affords a coating with high water resistance.<sup>30</sup> The contact angles of the UV-WFPUA films are shown in Fig. 3. The contact angle

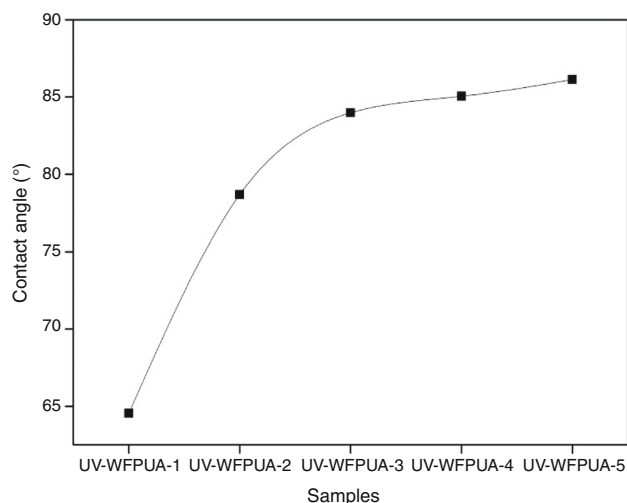


Fig. 3: Contact angles of the UV-WFPUA films

curve exhibits an increasing trend, which may be due to the C-F chain on the film surface. Due to its low surface free energy and surface tensions, the surface structure and the bulk structures differ. Therefore, the C-F chain segment transferred easily to the surface of the composite film.<sup>31</sup> The contact angle of the UV-WFPUA-1 film was  $64.55^\circ$ , which increased to approximately  $85^\circ$  after the introduction of HFBMA. The results also indicate that the sample surface will become more hydrophobic as the HFBMA content in the hybrid films increases. The prepared fluoropolymer possesses both hydrophobic and hydrophilic groups. Therefore, the contact angle of the sample increased but did not exceed  $90^\circ$ . When the content of HFBMA exceeded 10%, the contact angle of the membrane increased slowly, and this result was consistent with the change in water absorption shown in Table 3. Therefore, a HFBMA content of approximately 10% of the total mass of the system is desirable and corresponds to the UV-WFPUA-3 film.

### SEM of the UV-WFPUA films

Scanning electron microscopy (SEM) images of the fracture surface of the UV-WFPUA-1 and UV-WFPUA-3 films are shown in Fig. 4. The results indicate that the section without HFBMA is smooth, and the section with HFBMA is rough. Moreover, various size and shape protrusions were observed in the UV-WFPUA-3 section. As the water evaporates in the system, the concentration of fluorine-containing group increased during the film forming process. The fluorine-containing group transferred toward the film surface and the phenomenon of microfascies separation occurred. The chemical structure of fluorocarbon side chains differed with the soft and hard segments, which could cause incompatibility, thus leading to the formation of bumps on the film surface. Furthermore, no cracks were observed in the two sections, indicating that the WPUA oligomer, HFBMA monomer, and reactive diluents reacted to produce crosslinking reactions in Darocur 1173.

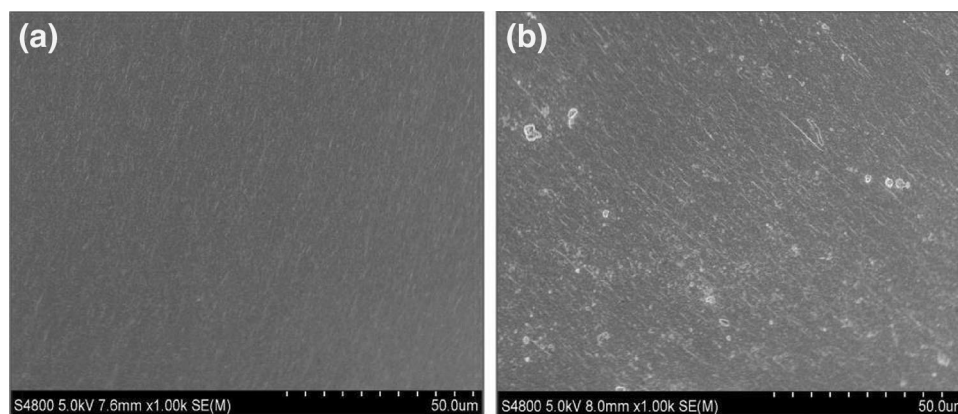


Fig. 4: SEM photographs of the UV-WFPUA-1 (a) and UV-WFPUA-3 (b) films

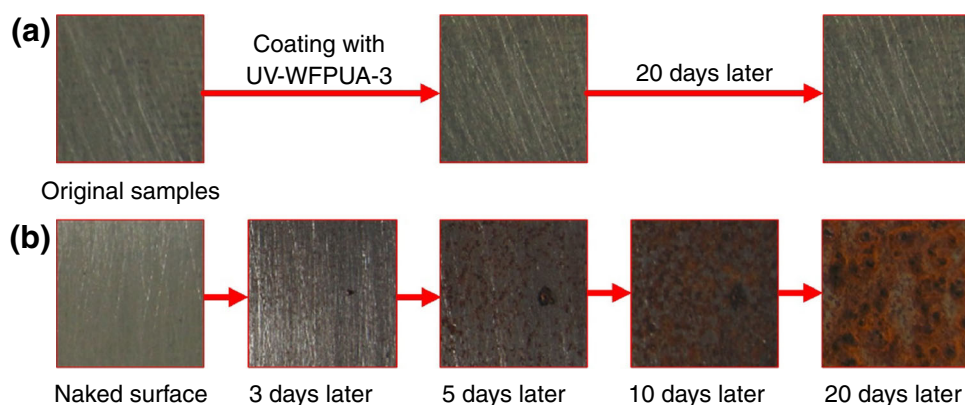


Fig. 5: Images of the iron sheet with UV-curable film coating (a) and naked metal surface (b)

### Application of the UV-WFPUA material

The most economical and effective method for coating protection of iron relics involved exposure to outdoor conditions. Based on the performance of the UV-WFPUA materials, the UV-WFPUA-3 emulsion was chosen as the protective coating for additional application studies. One iron sheet was coated with the UV-WFPUA-3 emulsion and cured using a UV lamp for 30 s, and the other iron sheet was used as a reference object. Figure 5 shows the change in the physical appearance of the sample surface. As shown in Fig. 5, no significant change in the surface of the iron sheet sample was observed. However, the iron sheet sample exhibited corrosion effects 3 days later and was seriously corroded after 20 days. The untreated iron sheet possessed a rusty texture, and the original surface was barely visible. This result indicated that the UV-WFPUA-3 emulsion exhibited excellent protective behavior and can be used as a protective material for iron relics.

### Conclusion

A series of UV-WFPUA coatings were successfully fabricated. The results indicated that the hardness, tensile strength, gel content, and contact angle increased as the HFBMA content increased. Furthermore, the SEM analysis revealed that the fracture surface of the UV-WFPUA-3 film contained no cracks and had a good crosslinked structure. Based on the overall performance of the prepared coating and application costs, the optimal amount of HFBMA that should be added was 10%, and UV-WFPUA-3 was selected for use as a protective coating. In addition, the result indicates that the UV-WFPUA-3 emulsion exhibited excellent protective behavior and can be used as a protective material for simulated iron relics.

**Acknowledgments** This project was supported by Natural Science Foundation of Jiangsu Province

(BK20161362 and BK20161264) and 333 High-Level Personnel Training Project of Jiangsu Province (BRA2016142).

### References

- Sultan, S, Kareem, K, He, L, "Synthesis, Characterization and Resistant Performance of Alpha-Fe<sub>2</sub>O<sub>3</sub>@SiO<sub>2</sub> Composite as Pigment Protective Coatings." *Surf. Coat. Technol.*, **300** 42–49 (2016)
- Baglioni, P, Chelazzi, D, Giorgi, R, Poggi, G, "Colloid and Materials Science for the Conservation of Cultural Heritage: Cleaning, Consolidation, and Deacidification." *Langmuir*, **29** 5110–5122 (2013)
- Baglioni, P, Berti, D, Bonini, M, Carretti, E, Dei, L, Fratini, E, Giorgi, R, "Micelle, Microemulsions, and Gels for the Conservation of Cultural Heritage." *Adv. Colloid Interf. Sci.*, **205** 361–371 (2014)
- Domingues, JAL, Bonelli, N, Giorgi, R, Fratini, E, Gorel, F, Baglioni, P, "Innovative Hydrogels Based on Semi-interpenetrating p(HEMA)/PVP Networks for the Cleaning of Water-Sensitive Cultural Heritage Artifacts." *Langmuir*, **29** 2746–2755 (2013)
- Totolin, MI, Neamtu, I, "Positive Findings for Plasma Polymer (Meth)acrylate Thin Films in Heritage Protective Applications." *J. Cult. Herit.*, **12** 392–398 (2011)
- Giussani, B, Monticelli, D, Rampazzi, L, "Role of Laser Ablation–Inductively Coupled Plasma–Mass Spectrometry in Cultural Heritage Research: A Review." *Anal. Chim. Acta*, **635** 6–21 (2009)
- Fernandes, P, "Applied Microbiology and Biotechnology in the Conservation of Stone Cultural Heritage Materials." *Appl. Microbiol. Biotechnol.*, **73** 291–296 (2006)
- Zhang, XY, Wen, WY, Yu, HQ, Chen, Q, Xu, JC, Yang, DY, Qiu, FX, "Preparation and Artificial Ageing Tests in Stone Conservation of Fluorosilicone Vinyl Acetate/Acrylic/Epoxy Polymers." *Chem. Pap.*, **70** 1621–1631 (2016)
- Cappelletti, G, Fermo, P, Camiloni, M, "Smart Hybrid Coatings for Natural Stones Conservation." *Prog. Org. Coat.*, **78** 511–516 (2015)
- Leyssens, K, Adriaens, A, Dowsett, MG, Schotte, B, Oloff, I, Pantos, E, Bell, AMT, Thompson, SP, "Simultaneous In Situ Time Resolved SRARD and Corrosion Potential Analyses

- to Monitor the Corrosion on Copper.” *Electrochem. Commun.*, **7** 1265–1270 (2005)
11. Vidakovic, AM, Ranogajec, JG, Markov, SL, Loncar, ES, Hirsberger, HM, Skapin, AS, “Synergistic Effect of the Consolidant and the Photocatalytic Coating on Antifungal Activity of Porous Mineral Substrates.” *J. Cult. Herit.*, **24** 1–8 (2017)
  12. Carretti, E, Dei, L, Baglioni, P, “Solubilization of Acrylic and Vinyl Polymers in Nanocontainer Solutions. Application of Microemulsions and Micelles to Cultural Heritage Conservation.” *Langmuir*, **19** 7867–7872 (2003)
  13. Wang, YY, Qiu, FX, Xu, BB, Xu, JC, Jiang, Y, Yang, DY, Li, PL, “Preparation, Mechanical Properties and Surface Morphologies of Waterborne Fluorinated Polyurethane-Acrylate.” *Prog. Org. Coat.*, **76** 876–883 (2013)
  14. Shendi, HK, Omrani, I, Ahmadi, A, Farhadian, A, Babnejad, N, Nabid, MR, “Synthesis and Characterization of a Novel Internal Emulsifier Derived from Sunflower Oil for the Preparation of Waterborne Polyurethane and Their Application in Coatings.” *Prog. Org. Coat.*, **105** 303–309 (2017)
  15. Li, R, Shan, ZH, “Research on Structural Features and Thermal Conductivity of Waterborne Polyurethane.” *Prog. Org. Coat.*, **104** 271–279 (2017)
  16. Dai, YT, Qiu, FX, Wang, LL, Zhao, JL, Yang, DY, Kong, LY, Yu, ZP, Yang, PF, “Effect of Different Photoinitiators on the Properties of UV-Cured Electromagnetic Shielding Composites.” *J. Polym. Eng.*, **35** 209–222 (2015)
  17. Dai, YT, Qiu, FX, Wang, LL, Zhao, JL, Yu, ZP, Yang, PG, Yang, DY, Kong, LY, “UV-Curable Electromagnetic Shielding Composite Films Produced Through Waterborne Polyurethane-Acrylate Bonded Graphene Oxide: Preparation and Effect of Different Diluents on the Properties.” *e-Polymers*, **14** 427–440 (2014)
  18. Park, JM, Jeon, JH, Lee, YH, Lee, DJ, Park, H, Chun, HH, Do Kim, H, “Synthesis and Properties of UV-Curable Polyurethane Acrylates Containing Fluorinated Acrylic Monomer/Vinyltrimethoxysilane.” *Polym. Bull.*, **72** 1921–1936 (2015)
  19. Qiu, FX, Xu, HP, Wang, YY, Xu, JC, Yang, DY, “Preparation, Characterization and Properties of UV-Curable Waterborne Polyurethane Acrylate/SiO<sub>2</sub> Coating.” *J. Coat. Technol. Res.*, **9** 503–514 (2012)
  20. Zhang, XY, Wen, WY, Yu, HQ, Qiu, FX, Chen, Q, Yang, DY, “Preparation, Characterization of Nano-silica/Fluoroacrylate Material and the Application in Stone Surface Conservation.” *J. Polym. Res.*, **23** 75 (2016)
  21. Li, PL, Qiu, FX, Zhang, XY, Wang, LL, Chen, Q, Yang, DY, “Preparation and Application of Fluorinated-Siloxane Protective Surface Coating Material for Stone Inscriptions.” *J. Polym. Eng.*, **35** 511–522 (2015)
  22. Çanak, TÇ, Serhatlı, İE, “Synthesis of Fluorinated Urethane Acrylate Based UV-Curable Coatings.” *Prog. Org. Coat.*, **76** 388–399 (2013)
  23. Zhang, CY, Zhu, ZW, Gong, SL, “Synthesis of Stable High Hydroxyl Content Self-Emulsifying Waterborne Polyacrylate Emulsion.” *J. Appl. Polym. Sci.*, **134** 44844 (2017)
  24. Kotlík, P, Doubravová, K, Horálek, J, Kubáč, L, Akrman, J, “Acrylic Copolymer Coatings for Protection Against UV Rays.” *J. Cult. Herit.*, **15** 44–48 (2014)
  25. Cano, E, Bastidas, DM, Argyropoulos, V, Fajardo, S, Siatou, A, Bastidas, JM, Degriñy, C, “Electrochemical Characterization of Organic Coatings for Protection of Historic Steel Artefacts.” *J. Solid State Electrochem.*, **14** 453–463 (2010)
  26. Xu, JC, Rong, XS, Chi, TY, Wang, M, Wang, YY, Yang, DY, Qiu, FX, “Preparation, Characterization of UV-Curable Waterborne Polyurethane-Acrylate and the Application in Metal Iron Surface Protection.” *J. Appl. Polym. Sci.*, **130** 3142–3152 (2013)
  27. Park, JM, Lee, YH, Park, H, Kim, HD, “Preparation and Properties of UV-Curable Fluorinated Polyurethane Acrylates.” *J. Appl. Polym. Sci.*, **131** 40603 (2014)
  28. Xu, JC, Qiu, FX, Rong, XS, Dai, YT, Yang, DY, “Preparation and Surface Pigment Protection Application of Stone Substrate on UV-Curable Waterborne Polyurethane-Acrylate Coating.” *J. Polym. Mater.*, **31** 287–303 (2014)
  29. Jeon, JH, Park, YG, Lee, YH, Lee, DJ, Kim, HD, “Preparation and Properties of UV-Curable Fluorinated Polyurethane Acrylates Containing Crosslinkable Vinyl Methacrylate for Antifouling Coatings.” *J. Appl. Polym. Sci.*, **132** 42168 (2015)
  30. Toniolo, L, Poli, T, Castelvetro, V, Manariti, A, Chiantore, O, Lazzari, M, “Tailoring New Fluorinated Acrylic Copolymers as Protective Coatings for Marble.” *J. Cult. Herit.*, **3** 309–316 (2002)
  31. Sheng, JL, Li, Y, Wang, XF, Si, Y, Yu, JY, Ding, B, “Thermal Inter-Fiber Adhesion of the Polyacrylonitrile/Fluorinated Polyurethane Nanofibrous Membranes with Enhanced Waterproof-Breathable Performance.” *Sep. Purif. Technol.*, **158** 53–61 (2016)